



Special Feature: Analytic Technologies of Powertrain

Research Report

A Study of Fuel Economy Improvements, and the Degradation and Recovery of Reforming Catalysts, in Engine EGR Reforming Based on Steam Reforming Fueled by Ethanol-blended Gasoline

Susumu Nagano

Report received on May 15, 2016

■**ABSTRACT**■ Engine exhaust-gas recirculation (EGR) reforming was experimentally investigated with a 2.4 L spark ignition internal combustion engine to improve the fuel efficiency of ethanol-blended gasoline-based engines. Using pure ethanol improved the fuel efficiency and allowed engine EGR reforming to be carried out at lower temperatures compared with gasoline. Using E85 (a mixture of 85% ethanol and 15% gasoline), the hydrogen concentration in the reforming gas increased with the use of an optimized catalyst. Performance degradation and recovery by steam reforming activation were also examined using test pieces of Rh catalysts. Hydrogen generation was maintained despite the presence of sulfur when oxygen, which was found to remove the carbon from the catalyst, was supplied during the recovery procedure. Therefore, the cause of the performance degradation was found to be not sulfur but carbon. The oxygen concentration and temperature were confirmed to decrease during recovery with the use of an improved catalyst carrier (CZA: ceria-zirconia-alumina). When a Rh/CZA catalyst was employed, even if the hydrogen concentration fell due to the use of gasoline, the hydrogen producing performance could be recovered through the use of E85. We were able to confirm 70 hours of use without degradation of the hydrogen producing performance.

■**KEYWORDS**■ Heat Engine, Fuel/alternative, Fuel Reforming, Steam Reforming, Ethanol, E85, EGR, Reforming Catalyst, Energy Recovery

1. Introduction

Ethanol, the paradigmatic example of a biofuel, is used both as a replacement for and as an additive to gasoline, and a variety of initiatives have sought to produce ethanol in Japan.^(1,2) As is widely known, ethanol is used as a replacement fuel in Brazil, while the high-ethanol-content blended gasoline known as E85 (a mixture of 85% ethanol and 15% gasoline; in what follows, we will use the notation EX to denote blends consisting of X% ethanol and the remainder gasoline) is used in North America, Thailand, and Sweden. In addition, an increasing number of overseas nations recommend E20. In Japan, the low-ethanol-content blended gasoline E3 is used, and E10-compatible vehicles are becoming increasingly more common.

In this report, we discuss two items: (a) experiments and practical tests involving prototype gasoline engines designed to improve fuel economy by ethanol-blended gasoline steam reforming, and (b) an analysis of the factors responsible for the degradation and recovery of reforming catalysts – which play an important role

in steam-reforming performance – and a new recovery method that we propose based on this analysis.

Although the blend ratio of fuels available in the marketplace is typically determined by the volume ratio, in this report, we instead used the mass ratio. The reasons for this are: (1) the specific masses of gasoline and ethanol are similar and exhibit little variation as the blend of the two ingredients varies, and (2) using the mass ratio allows for accurate measurements even for small quantities.

Gasoline steam reforming engines have been a focus of research and development efforts as candidate technologies offering improved thermal efficiency via two mechanisms: (1) enhanced fuel economy from the hydrogen produced by hydrocarbon fuels, and (2) recycling of waste heat due to the fuel-steam-reforming reaction, which is an endothermic reaction that takes place at the time of hydrogen production.^(3,4) However, practical applications of this technology to internal combustion engines are said to be out of reach due to a host of technical difficulties, including (a) the fact that the temperature of the exhaust gas must exceed

600°C when using gasoline, and (b) the catalytic corrosion due to sulfur present in gasoline, which causes the activity to decline in a short period of time; recovery requires both lengthy time intervals and exposure to a high-temperature environment, leading to thermal degradation.⁽⁵⁾ Research and development efforts to use ethanol reforming as a hydrogen source for fuel cells employ partial-oxidation reforming methods based on internal heat generation, i.e., the autothermal reforming process;^(6,7) these emphasize start-up performance instead of waste-heat recovery and would be difficult to apply to fuel-economy improvements in internal combustion engines.

In a previous study,⁽⁷⁾ we conducted test-piece experiments based on exhaust-gas recirculation (EGR) in internal combustion engines fueled by ethanol. We demonstrated that fuel-steam reforming using the steam in EGR allows the reforming reactions to proceed out of equilibrium at relatively low temperatures, increasing the quantity of hydrogen produced and yielding significant gain in the reforming process. In this paper, we refer to this as the rate of increase of lower heating value. This result indicates that hydrogen offers improved combustion compared to conventional approaches, allowing the quantity of EGR introduced to be increased, and is highly likely to yield improved fuel economy due to reduced pumping loss under partial loading.

In addition, we have previously studied the activity of Rh catalysts for hydrocarbon steam reforming and how it is affected by the use of (a) iso-octane and (b) gasoline containing a sulfur concentration on the order of 6 ppm.⁽⁷⁾ The results indicated that when sulfur is present in the fuel, the activity began to decrease within 10 hours, even at a high temperature of 750°C. In contrast, for iso-octane, which does not contain sulfur, there was essentially no observable decline in activity even at 600°C.⁽⁸⁾ At that time, we concluded that sulfur contributes significantly to degradation. In this study, we create a honeycomb structure for the reforming catalytic medium used for test pieces. We divide the catalytic medium into three sectors, from upstream to downstream, and for each sector, we analyze the factors contributing to decreased activity, focusing in particular on the quantities of sulfur and carbon, which would be expected to increase as activity decreases. We also study methods for recovering catalytic activity. Finally, we address the question of degradation and recovery when gasoline is used.

2. EGR Reforming in an Inline Engine

In this section, we report experiments and practical tests of ethanol-blended gasoline steam reforming to improve the fuel economy of a 2.4 L inline engine. Because the process of fuel steam reforming is an endothermic reaction for both the fuel and the steam, it requires a source of heat. In this study, we used the steam in EGR as a steam source and realized the heat source via thermal exchange with the exhaust gas.

Figure 1 shows a schematic diagram of the system. Fuel for reforming is injected into EGR extracted from the front of the ternary catalyst to yield the base gas for reforming. The exhaust gas is mixed with a crossflow of this base gas in a heat-exchange reformer to induce heat exchange. The exhaust gas cools due to the heat exchange and is emitted as exhaust. The base gas, which is reformed by the reforming catalyst, becomes a hydrogen-containing reformed gas and passes through the EGR valve to blend with the absorbed air. For the reforming catalyst in this step, we initially used an Rh catalyst with a CaZrO₂ carrier, as discussed below.

2.1 Comparing the EGR Steam-reforming Properties of Ethanol and Gasoline

Figure 2 compares the temperature characteristics for the cases in which ethanol and gasoline are used as the reforming fuel. To ensure that only the temperature characteristics of the reforming process for different fuels were being compared, we used ethanol as the primary fuel in both cases, varying only the fuel used for reforming. In this figure, the horizontal axis is the

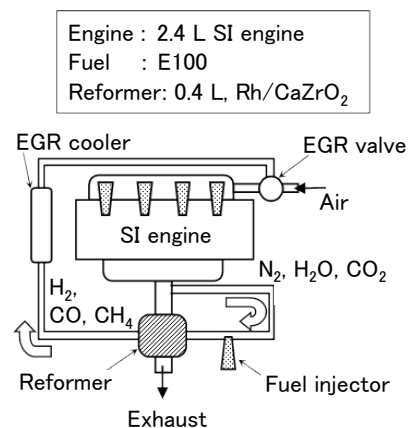


Fig. 1 EGR fuel steam reforming system on spark ignition internal combustion engine with reformer.

engine exhaust temperature, and the quantity of fuel used for reforming is fixed. The exhaust temperature was adjusted by varying the engine speed (rpm) and the brake mean effective pressure (measured in MPa; denoted by P_{me} in Fig. 2 and subsequent figures) as parameters.

We see that changing the reforming fuel from gasoline to ethanol allows a reduction of more than 150°C in the exhaust-gas temperature required to achieve the same hydrogen concentration. Considering the regime of temperatures below 600°C , we see that the quantity of hydrogen produced with ethanol is roughly 3 times greater than that produced with hydrogen at 400°C , and more than 2 times greater at 500°C .

2.2 The Effect of EGR Reforming on Improved Fuel Economy

Figure 3 shows the dependence of EGR reforming properties on the amount of fuel injected. Here, ethanol was used as both the primary injection fuel and the reforming fuel. Tests were conducted at EGR ratios (denoted EGR in the figure) of 20% and 28%. The horizontal axis shows the ratio of reforming fuel to total supply fuel (the sum of the quantities of primary injection and reforming fuel), allowing the determination of the optimal allocation of fuel to the reforming process.

The temperature distribution of the catalytic bed – both near the inlet and near the center – does not change as the EGR ratio is varied. This indicates that variations in the EGR ratio do not change the temperature at which the endothermic reaction

due to the reforming process is in balance with the supply heat supplied by the exhaust gas. When the ratio of reforming fuel increases, the volume of the endothermic reaction increases, reducing the internal temperature of the reformer and increasing the production of hydrogen. As the quantity of reforming fuel increases, the temperature decreases despite the heat supplied by the exhaust gas. This causes a drop in catalytic activity, retarding the reforming reaction and reducing the quantity of hydrogen production. Thus, there exists an optimal ratio of fuel to be allocated to the reforming process to yield maximal improvement in fuel economy. In this case, the optimal allocation ratio is approximately 25%.

Figure 4 shows the effect of the EGR ratio on fuel economy. To minimize losses associated with pumping, it is desirable to choose high EGR ratios; however, under ordinary conditions, increasing the EGR ratio reduces the flame propagation speed and creates combustion instabilities. Therefore, there exists an optimal EGR ratio that maximizes fuel economy. However, if EGR reforming yields large quantities of hydrogen in EGR gas, then increasing the EGR ratio may allow this threshold to be exceeded, yielding stable combustion and improving fuel economy. From Fig. 4, we see that in the absence of reforming, fuel economy is optimized at an EGR ratio of 21%, whereas the use of reforming increases this ratio to as

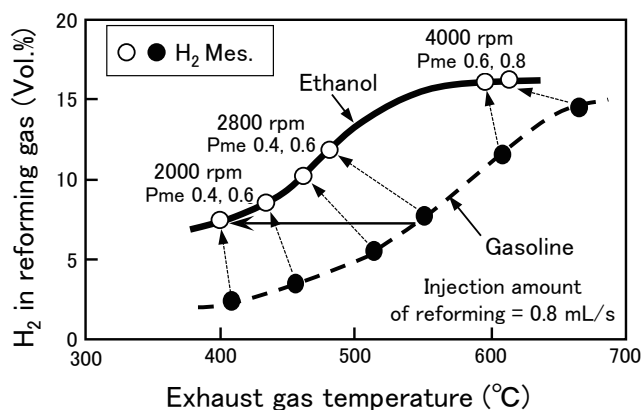


Fig. 2 Hydrogen generation properties of EGR fuel steam reforming system on spark ignition internal combustion engine.

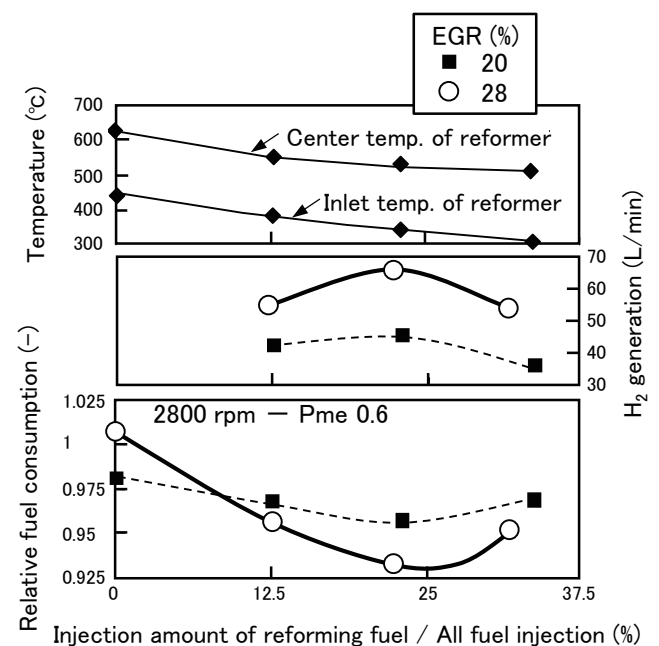


Fig. 3 Effect of injection amount of reforming fuel on fuel consumption and hydrogen generation properties.

high as 28%. We attribute this to the effect of hydrogen in improving the flame propagation speed. The use of reforming allows a dramatic increase in the EGR ratio, resulting in a 4.6% improvement in fuel economy. The increased rate of heat production due to the recycling of waste heat presumably also contributes to the improved fuel economy, but we were not able to establish a clear separation between the effects of these two mechanisms.

2.3 Hydrogen-production Performance in EGR Reforming Using E85 Fuel

Figure 5 compares the hydrogen concentration of reforming gas in engine EGR reforming with E85, a high-ethanol-concentration blended gasoline, used as both the primary injection fuel and the reforming fuel.

The figure shows the hydrogen concentration for two reforming catalysts: the catalyst we have used thus far in this paper (with CaZrO_2 carriers) and a reforming catalyst to be discussed below (with

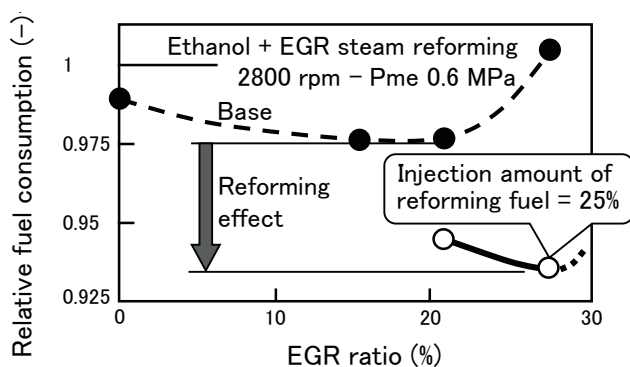


Fig. 4 Effect of EGR ratio on fuel consumption.

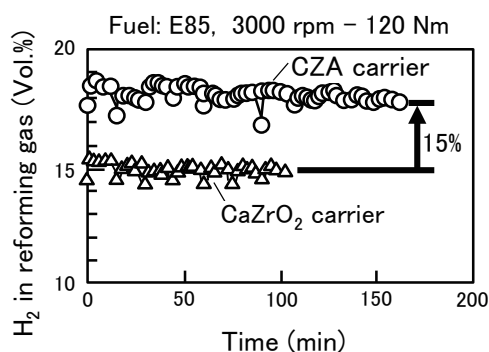


Fig. 5 Effect of catalyst carriers on EGR steam reforming system for E85 fuel mixed with gasoline (S = 34 ppm).

CZA carriers). Although we have focused thus far on ethanol, in this case we attempted EGR reforming using the high-ethanol-concentration gasoline blend E85 to investigate whether or not our findings could be extended to a broader range of applications. Because the temperature of the exhaust gas was approximately 500°C , we feared that the catalytic activity would decline after 1-2 hours of use in the reforming process due to sulfur contamination, as discussed above. However, in neither case did we observe a significant decrease in activity. We observed adequate hydrogen-producing performance both for Rh catalysts with CaZrO_2 as carriers and Rh catalysts with CZA as carriers, indicating that, as discussed below, the reforming catalysts that yield high performance in test pieces also exhibit high performance in engine EGR reforming. However, the absolute magnitudes of the hydrogen concentrations differ for test pieces and for engine experiments. We suspect that the factors responsible for this phenomenon include (a) the removal of carbon deposits near the catalyst inlet due to trace quantities of oxygen in engine exhaust (the same phenomenon as the recovery process discussed below) and (b) the temperature distribution in the regions experiencing the reform reaction; however, we have not investigated this point in detail and leave it as a topic for future study.

Using CZA as a carrier for catalysts yielded an increase of 15% in the hydrogen concentration relative to the use of CaZrO_2 as a carrier. This finding suggests that the use of CZA as a carrier may promise further improvements in fuel economy. We will discuss in detail the factors responsible for our finding that the use of E85 did not result in a significant decrease in catalytic activity in the subsequent sections.

3. Selection of Steam-reforming Catalysts and Their Degradation/recovery

3.1 Selection of Reforming Catalysts

We began by conducting a survey of types of catalyst by using various types of pellet catalyst in fixed-bed flow reaction tube experiments with ethanol as a fuel. **Table 1** shows the results of this survey. The leftmost column in this table is the reforming catalyst, while the column to its right indicates the base substance or its features and preparer. The experimental conditions

were configured as follows: reactor temperature of 400°C, S/C (steam/carbon mole ratio) = 1, N₂ dilution, and space velocity of 60000-80000/h for the gas as a whole.

To organize our results, we introduce a number of quantities defined by the following equations.

$$\text{Decomposition} = \left(\sum [\text{Concentration of all C-containing output gas, excluding ethanol, normalized to C} = 1] \times \text{molar flow volume of output gas} \right) / \left(\text{molar flow volume of added ethanol} \times 2 \right) \times 100 (\%) \quad (1)$$

$$\text{Rate of increased heating value (R/Et)} = \left(\sum [\text{heating value for each component of the output gas}] - \text{heating value for added ethanol} \right) / \left(\text{heating value for added ethanol} \right) \times 100 (\%) \quad (2)$$

$$\text{Heating value rate for each gas (H}_2\text{/Et, CO/Et, CH}_4\text{/Et)} = \text{heating value for each component of the output gas} / \text{heating value for added ethanol} \times 100 (\%) \quad (3)$$

Here, “output gas” refers to dry gas, while “heating value” means the lower heating value.

Gas compositions were measured via gas chromatography (using a thermal-conductivity detector). Each measurement required approximately 30 minutes, during which time we also estimated the decrease in activity due to factors such as carbon deposits from observed variations in the flow volume of reforming gas.

With Rh used as the metal catalyst, high values for both the decomposition and the rate of increased heating value were observed for ceria-based and zirconia-based catalysts. In particular, the ceria (CA; CeO₂-Al₂O₃)⁽⁹⁾ catalyst yielded large values for both the rate of increased heating value and the decomposition. For the ceria-carried catalyst, the quantity of Rh supported changed to 1 wt% and 3 wt% (mass fraction relative to carriers). Using a larger quantity of Rh yields higher values for the decomposition but does not improve the rate of increased heating value. The reason for this is that, as

Table 1 Results of activation for various catalysts at furnace temperature = 400°C: [R] means R/Et and [D] means decomposition.

Catalyst	Material or Characteristics /Maker	Increase of heating value [R] and decomp. [D/10] (%)		Remark
		0	10	
Rh (3 wt%) /CaZrO ₂	CaZrO ₂ : Basic carrier /Daiichi Kigenso Kagaku Co. Cat. /Toyota CRDL., Inc.	R: ~7.5 D: ~4.5		Little coking
Rh (1 wt%) /CeO ₂	CeO ₂ : Basic carrier /Daiichi Kigenso Kagaku Co. Cat. /Toyota CRDL., Inc.	R: ~7.5 D: ~2.5		Little coking
Rh (3 wt%) /CeO ₂	CeO ₂ : Basic carrier /Daiichi Kigenso Kagaku Co. Cat. /Toyota CRDL., Inc.	R: ~7.5 D: ~5.5		Little coking
Rh (3 wt%) /α-Al ₂ O ₃	α-Al ₂ O ₃ : Basic carrier /Showa Electric Co. Cat. /Toyota CRDL., Inc.	R: ~5.5 D: ~2.5		No coking
Rh (3 wt%) /CeO ₂ -Al ₂ O ₃	Modified ceria /Toyota CRDL., Inc.	R: ~7.5 D: ~8.5		No coking
Ni (10 wt%) /Al ₂ O ₃	Methane steam reforming /Toyota CRDL., Inc.	R: ~7.5 D: ~7.5	Carbon deposition over 350°C	Coking over 350°C
Cu (15 wt%) /ZnO	Methanol steam reforming /Süd-chemie Catalysts	R: ~7.5 D: ~6.5		Sintering over 350°C
Pd (0.5 wt%) /Al ₂ O ₃	Olefin hydrogenation /Süd-chemie Catalysts	R: ~7.5 D: ~7.5	No activation at 400°C	Coking at 650°C
Ru (2 wt%) /Al ₂ O ₃	Steam reforming /Süd-chemie Catalysts	R: ~7.5 D: ~7.5	No activation at 400°C	No coking

the activation point increases, the decomposition of the raw materials proceeds, but the fraction of methane produced is greater than the fractions of hydrogen or CO produced. Thus, for Rh catalysts, it is important to optimize the quantity of Rh supported.

Nickel catalysts, which are suitable for methane steam reforming, have the property that upon entering the temperature regime in which they begin to exhibit activity, the sedimentation of carbon deposits simultaneously becomes severe under the condition of $S/C = 1$, clogging the reaction tube within minutes. Copper catalysts, which are suitable for methanol steam reforming, exhibit high hydrogen-producing performance and high decomposition, but above 350°C they exhibit a decrease in activity within a few hours, which is believed to be caused by sintering. For commercially available Pd and Ru catalysts, we observed no activity at 400°C . For Pd catalysts, in the range $600\text{--}650^{\circ}\text{C}$ ethanol decomposed into ethylene and steam, at which point the sedimentation of carbon deposits again became severe.

Next, we fixed the catalyst at Rh and investigated the effect of varying the carrier. **Figure 6** shows the heat evolved by gas produced with a fixed volume of Rh with alumina-based, ceria-based, and zirconia-based carriers. The primary component of others is non-reactive ethanol; when this substance is scarce, values of the decomposition are high.

Substances with little acid-point volume are said to be well-suited for use as steam-reforming catalysts.

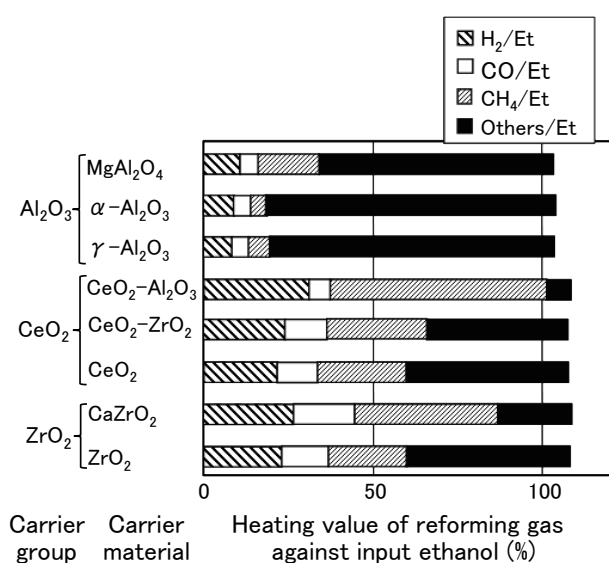


Fig. 6 Comparison of heating values of reforming gas for various catalyst carriers at 400°C , $S/C = 1$, N_2 dilution and $\text{Rh} = 3 \text{ wt}\%$ against carrier weight.

Alumina is generally a carrier with much acid-point volume, whereupon it yielded little increase in the quantity of heat produced. Ceria-based carriers overall exhibited large increases in the heating value. CA carriers give rise to large volumes of hydrogen production, large volumes of methane production, and high values of the decomposition. We attribute this to the low acid-point volume of CeO_2 , promoting conversion to methane via interactions between ceria and alumina. The production of methane from hydrogen and CO is a heat-producing reaction, which serves to mitigate the temperature decrease compared to cases involving only endothermic reactions and allows the ethanol decomposition reaction to proceed. Zirconia-based systems also have low acid-point volume, and for these carriers also we observed large increases in heating value, essentially equivalent to that of the ceria carriers.

Based on these results of our evaluation of activity rates, we conclude that ceria-based carriers are optimal for the goal of increasing heating value, with zirconia-based carriers a close second, while catalysts with CA carriers are optimal from the goal of increasing decomposition values.

For CZA ($\text{CeO}_2\text{-ZrO}_2\text{-Al}_2\text{O}_3$) carriers,^(10,11) which we found could offer even larger improvement in the rate of increased heating value than ceria carriers (CA: $\text{CeO}_2\text{-Al}_2\text{O}_3$), **Figure 7** shows the temperature dependence of the heat generated by the gas produced using a reforming catalyst in which the volume of Rh

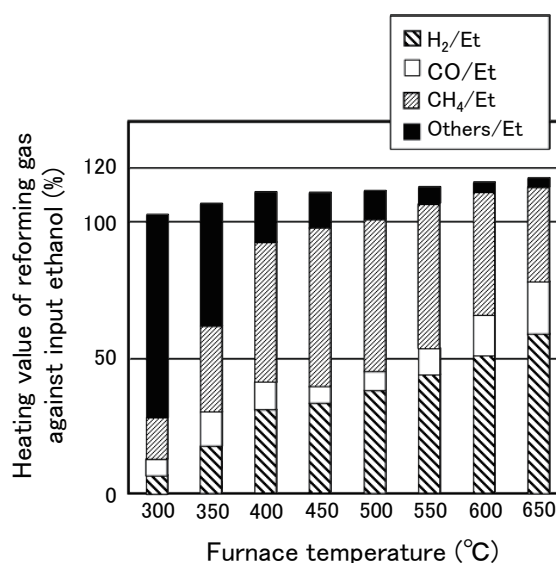


Fig. 7 Change of heating values of reforming gas with CZA catalyst carriers at 400°C , $S/C = 1$, N_2 dilution and $\text{Rh} = 2 \text{ wt}\%$ against carrier weight.

supported was optimized. Note that CZA is a carrier consisting of CA with some of the ceria replaced by zirconia. The space velocity is approximately 70000/h for the entire gas. There is an increased rate of heating value for exhaust gas temperatures in the range of 300-650°C, corresponding to the temperature of the exhaust gas from the gasoline engine of an automobile during ordinary motion. This suggests that benefits may be readily obtained by applications to automotive engines.

3.2 Degradation and Recovery of Reforming Catalysts

Practical uses of catalytic bodies frequently involve honeycomb structures instead of palettes. In this section, we discuss test pieces prepared by coating cylindrical cordierite honeycomb structures with reforming catalyst.

3.2.1 Experimental Apparatus for Degradation and Recovery Tests

Figure 8 shows a schematic diagram of our experimental apparatus. Its specifications are listed below.

- Carrier gas: N₂-balanced CO₂ (13%) blended gas
- Vaporizer/mixer: An stainless tube of outer radius 12 mm and inner radius 10 mm is filled with brass beads of radius 3 mm with a static mixer internally installed.
- Electrical heater: Used to heat various units
- Gas flow meter: Wet gas meter (Shinagawa W-NK-1)
- Gas chromatograph: Shimadzu GC-8A with thermal conductivity detector (TCD)

- Apparatus for analyzing carbon and sulfur: Horiba EMIA920V
- High-temperature analyzer: Okura Riken TP5000 temperature programmed desorption (TPD)
- Locations of measurements: (A) center of catalytic bed, (B) outer walls of catalyst, (C) catalyst entry gas. Thermocouples are installed at each position.

3.2.2 Evaluation Procedure

Our experimental conditions are listed in **Table 2**. Our fuel is E85; we used two types of gasoline (with original sulfur concentrations of 34 ppm and 3 ppm) to yield two types of E85 blends (with sulfur concentrations of 5.0 ppm and 0.5 ppm, respectively). We now discuss our evaluation procedure.

With carrier gas flowing, we heated the furnace to 300°C, after which we began to add water. After the temperatures of the various units had stabilized, we began to supply fuel to initiate the reforming process. To analyze the reformed gas, we performed gas chromatography a total of 3 times, at intervals of 2 minutes, 9 minutes, and 16 minutes after the start of fuel supply. In view of limitations on the time available to analyze the reformed gas, we set the duration of the reforming process to 20 minutes 40 seconds. Then, we terminated the supply of fuel, waited for the temperature of the heated units to stabilize at the recovery temperature, initiated the recovery process, and terminated it after 15 minutes.

Counting the full process from the initial supply of fuel for reforming to the end of recovery as one reforming-recovery cycle, we repeated the process with similar analytical timing. To analyze the state of the catalysts, we ground the test pieces into powders

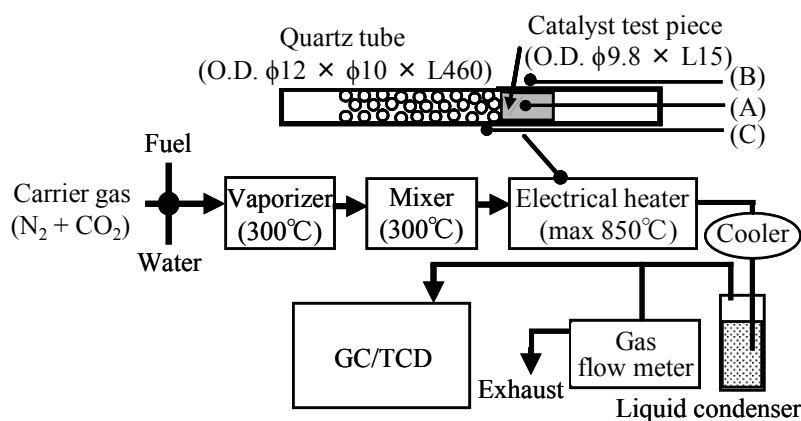


Fig. 8 Schematic diagram of experimental apparatus.

and performed carbon and sulfur analyses, as well as temperature programmed desorption analysis, for each unit. Repeating the cycle described above yielded the temporal variation in hydrogen concentration shown in **Fig. 9**.

3. 2. 3 Experimental Results

Defining the fuel addition time (measured in units of minutes) as the fraction of the full reforming-recovery cycle occupied by the reforming process, we focused on variations in hydrogen concentration, i.e., hydrogen-production performance, to characterize the influence of the various parameters.

3. 2. 3. 1 The Effect of Sulfur Concentration

Figure 10 shows results for fuel sulfur concentrations of 5.0 and 0.5 ppm. The table in the figure shows the quantity of sulfur that flowed in to the catalyst. Taking the volume of sulfur that flowed in 420 minutes after the start of fuel addition at a sulfur concentration of 5.0 ppm to be 1 (this quantity is denoted by (a) in the figure and below), the volume after 930 minutes at a sulfur concentration of 5.0 ppm was 2.2 (denoted (b) below), while at a sulfur concentration of 0.5 ppm the volumes after 420 and 1820 minutes were respectively 0.1 (denoted (c) below) and 0.4 (denoted (d) below). Comparing (a) and (c), we see that, despite the ten-fold

Table 2 Experimental conditions for CaZrO₂ carrier.

Catalyst	Rh (4.8 g/L) / ZrO ₂ -CaO (240 g/L)
Support	3 mil / 600 cpsi cordierite honeycomb
Volume	0.716 mL
Fuel	E85 (Sulfur 5.0 or 0.5 ppm) (Ethanol 85 wt% + Gasoline 15 wt%) (The amount of sulfur in gasoline is mixed 3 or 34 ppm)
S/C (Steam/Carbon mol ratio)	0.5, 1.0
GHSV	80000 h ⁻¹
Reforming temperature	600°C
Recovery temperature	550, 650, 750°C
O ₂ concentration (Recovery)	0, 1.0%

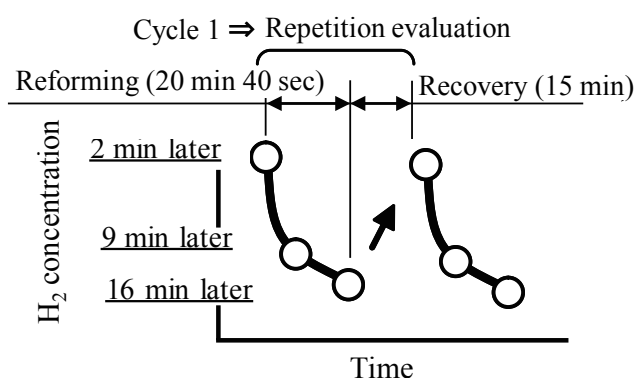


Fig. 9 Timing of gas sampling.

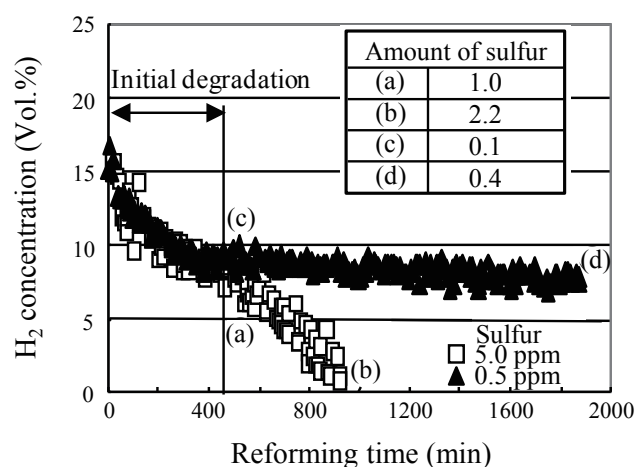


Fig. 10 Effect of sulfur concentration in fuel (reforming temp. 600°C, recovery temp. 650°C, S/C = 1.0).

difference in sulfur concentration, the two cases exhibit similar hydrogen-producing performance up to 400 minutes after the start of fuel addition. We consider this interval to constitute an inferior initialization stage that is independent of the quantity of sulfur flowed in. Thereafter, under the sulfur-rich conditions of (b), we find a sharp drop in hydrogen concentration, while under the sulfur-poor conditions of (d), we see a gentle decrease in hydrogen performance but a preservation of hydrogen-production performance.

Figure 11 shows the results of carbon and sulfur analyses after reforming at points (a), (b), (c), and (d) in Fig. 10. Both the carbon content and the sulfur content decrease from the front (Δ) to the center (\circ) to the rear (\square) of the catalytic site, i.e., from upstream to downstream. The amount of sedimentation of both carbon and sulfur increases over time and at the catalytic site, a large amount of sedimentation occurs

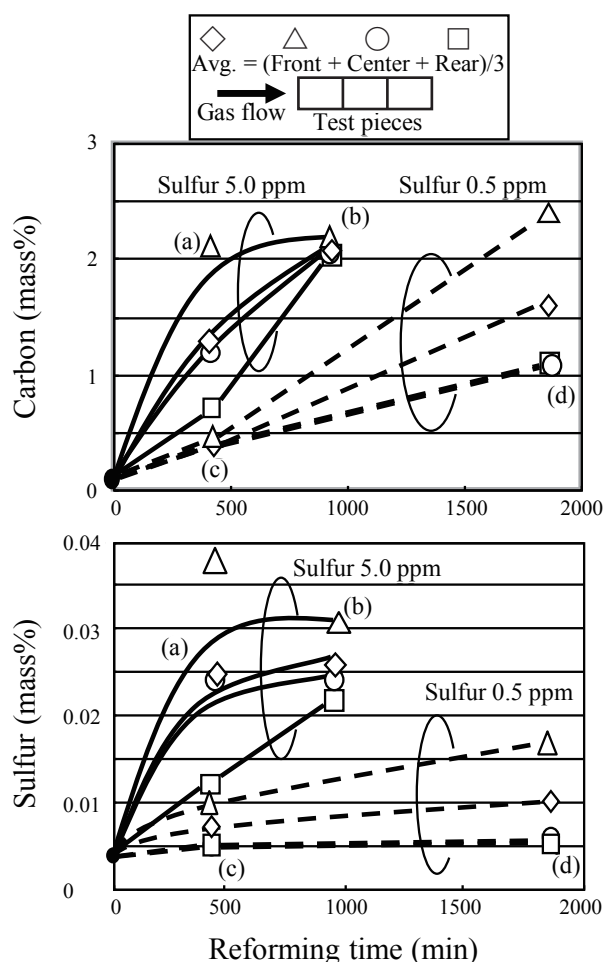


Fig. 11 Analysis result of carbon and sulfur of test pieces (reforming temp. 600°C, recovery temp. 650°C, S/C = 1.0).

upstream (Δ) at the beginning, and sedimentation occurs downstream (\circ , \square) thereafter. At point (b), where the hydrogen concentration approaches 0, the average carbon and sulfur content are respectively 2 wt% and 0.025 wt%, while at point (a) we have indications of a trend toward saturation for both carbon and sulfur. At point (c), both carbon and sulfur are scarce. Although the carbon content is 2.5 wt% prior to point (d), at intermediate and later stages, carbon is present in smaller quantities. Thus, because catalytic activity is present at both intermediate and later stages, the hydrogen-production performance was maintained for as long as 1820 minutes.

3. 2. 3. 2 Investigating the Conditions of the Recovery Procedure

Figure 12 shows the hydrogen concentration and the results of carbon and sulfur analyses, following reforming under identical conditions with the recovery procedure conducted 420 minutes after the start of fuel addition. Here, the recovery procedure was to vary the temperature to induce flow of carrier gas and steam. At high recovery temperatures, the hydrogen concentration is high, while carbon and sulfur are scarce. Maintaining catalysts at high temperatures typically causes fear of catalytic degradation due to sintering.

Figure 13 shows results quantifying the effect of supplying trace amounts of oxygen at a recovery temperature of 650°C as a means of lowering the recovery temperature. Air (1% oxygen equivalent) was

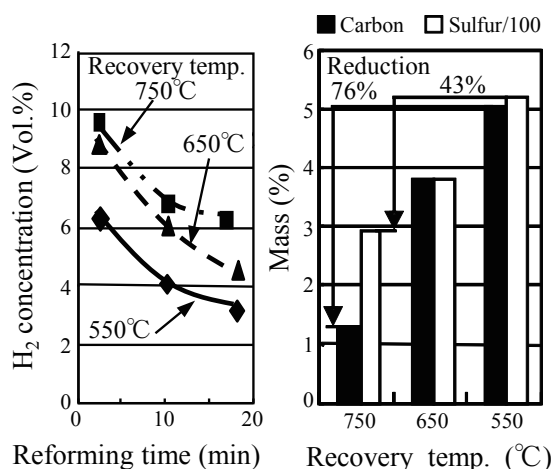


Fig. 12 Effect of recovery temperature (reforming temp. 600°C, sulfur 5.0 ppm, S/C = 0.5).

added during the recovery process. Under conditions in which oxygen is present during the recovery procedure, the extent of the recovery in the hydrogen concentration is significant, even for more than 500 minutes past the start of fuel addition, indicating the preservation of hydrogen-production performance.

Figure 14 shows the results of carbon and sulfur analyses after the recovery process. Here, we are comparing – for points A and B in Fig. 12 at a point 930 minutes after the start of fuel addition – results obtained with oxygen present and absent during recovery. With oxygen present, the carbon content falls

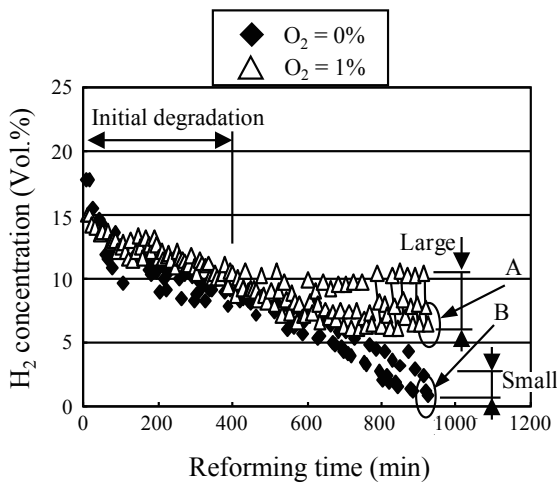


Fig. 13 Effect of oxygen supply during recovery (reforming temp. 600°C, recovery temp. 650°C, S/C = 1.0, sulfur 5.0 ppm).

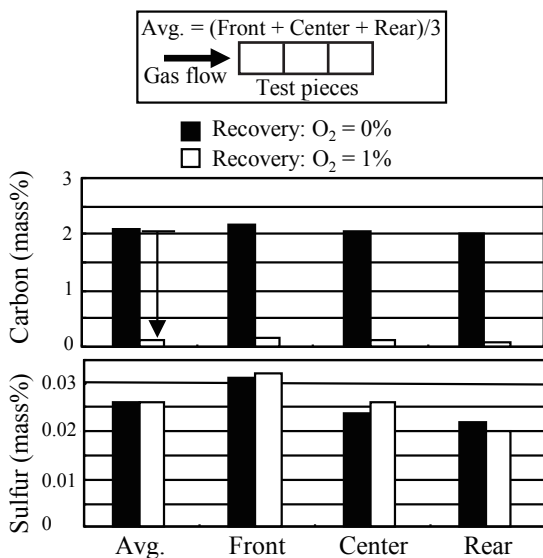


Fig. 14 Analysis result of carbon and sulfur of test pieces (reforming temp. 600°C, 930 min, recovery temp. 650°C, S/C = 1.0, sulfur 5.0 ppm).

by 93%, while the sulfur content does not decrease. This constitutes important evidence demonstrating that the recovery of catalytic activity despite the presence of sulfur.

3. 2. 3. 3 The Effect of Catalytic Carriers on the Conditions of the Recovery Process

We compared two catalyst carriers – the CZA (CeO₂-ZrO₂-Al₂O₃) carrier^(10,11) described above, and a CaZrO₂ carrier – from the perspective of degradation and recovery. Figure 15 shows the results of repeatedly performing the reforming-recovery procedure, under the conditions listed in Table 3, and comparing hydrogen concentration recovery rates to assess the effect of different catalyst carriers on degradation and recovery. At a recovery temperature of 650°C and a recovery time of 15 minutes, the hydrogen concentration recovery rate was 5 points higher for CZA carriers than for CaZrO₂ carriers even for zero oxygen concentration during recovery. Next, we compared the temperatures at which the recovery rate hit 100% for an oxygen concentration of 0.5% during recovery. For CaZrO₂ carriers, this temperature is 600°C, while for CZA carriers it is 550°C. Moreover, even at a recovery temperature of 500°C the recovery rate is over 95%. Figure 16 shows the results of carbon and sulfur analyses following a recovery procedure conducted 2130 minutes after the start of fuel addition. The average values of the carbon and

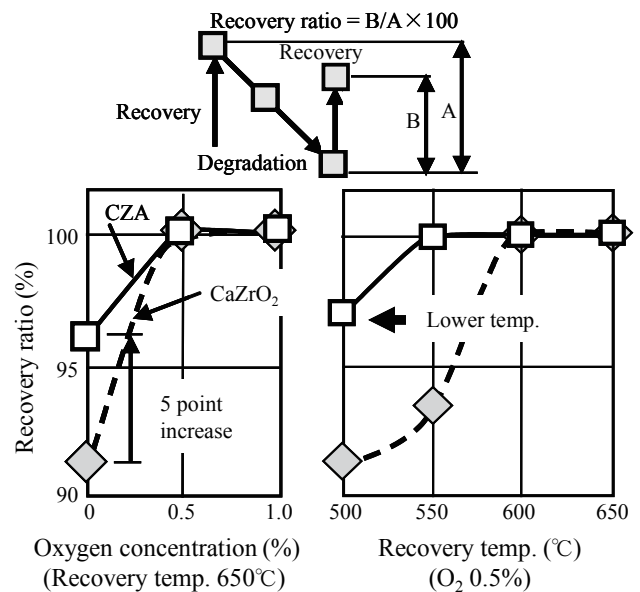


Fig. 15 Recovery ratio of hydrogen concentration.

Table 3 Experimental condition for CZA carrier.

Catalyst	Rh (4.8 g/L) / CZA (240 g/L)
Support	3 mil / 600 cpsi cordierite honeycomb
Volume	2 × 0.716 mL (two pieces)
Fuel	E85 (S = 5.0 ppm) (Ethanol 85 wt% + Gasoline 15 wt%)
S/C	1.0
GHSV	60000 h ⁻¹
Reforming temperature	600°C
Reforming time	20 min 40 sec
Recovery temperature	500, 550, 600, 650°C
Recovery time	5, 10, 15 min
O ₂ concentration (Recovery)	0, 0.5, 1.0, 1.5%

sulfur concentrations are respectively 70% and 45% lower for CZA carriers than for CaZrO₂ carriers.

Based on these findings, we expect that CZA carriers, for which one finds lower concentrations of carbon and sulfur to coat sites of catalytic activity, will allow hydrogen production performance to persist for longer times. Moreover, we have demonstrated that CZA carriers are useful for allowing relaxed recovery conditions (including lower temperatures and lower oxygen concentrations).

3.3 Assessing the Impact of Gasoline Concentration

In this section, we discuss the effect of gasoline concentration on hydrogen-production performance under repetition of the reforming-recovery procedure. The factor expected to be most important in governing the effect of varying gasoline concentration on the degradation and recovery process is the sulfur concentration.

To investigate sedimentation and exhaust of sulfur, we studied degradation and recovery at reforming times of 2100-4200 minutes for the test pieces shown in **Fig. 17** under the conditions of **Table 4**. During recovery, we used an SO₂ meter (of ultraviolet-absorption type) to detect SO₂, and we used an exhaust gas analyzer (of infrared-absorption type) to measure CO₂, THC, and CO. During the reforming process we used a detector tube (GasTec) to attempt measurements of H₂S and CS₂, but none was detected.

Figure 18 shows the results of measurements of the hydrogen concentration for fuels of varying gasoline concentrations, centered around E85 as indicated in the figure. Compared to E85, E20 exhibits lower hydrogen concentration and more rapid degradation of hydrogen-production performance; these problems

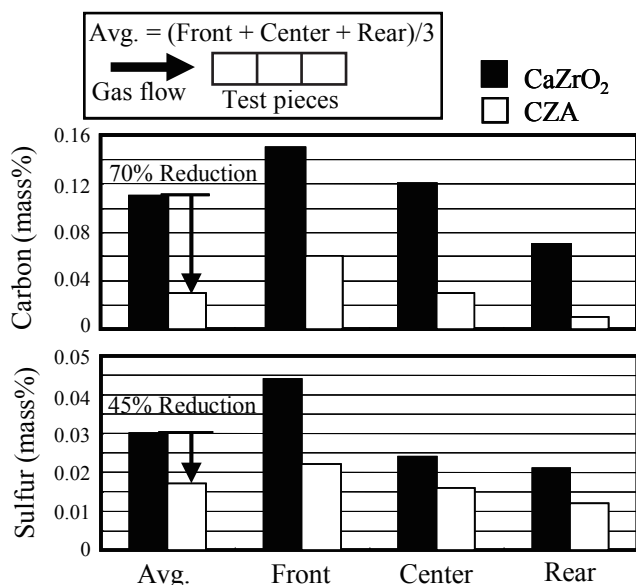


Fig. 16 Residual amount of carbon and sulfur after recovery (reforming temp. 600°C, recovery temp. 650°C, reforming: 2130 min).

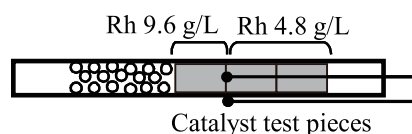


Fig. 17 Sketch of quartz tube set-up.

are mitigated by using E85. Next, gasoline has even lower hydrogen content than E20, and the degradation of its hydrogen-production performance proceeds immediately, but gradually recovers through the use of E85.

For gasoline, which exhibited low reforming activity, we performed a re-evaluation at a reforming temperature of 700°C after 3760 minutes. The hydrogen concentration was equivalent to that of E85, but degradation continued until the hydrogen concentration fell to 7.5%. At this point, using E85 again resulted in a gradual increase in hydrogen concentration, returning to the hydrogen concentration observed when E85 was used from the start. Based on

these findings, we conclude that the use of gasoline (containing a sulfur concentration of 34 ppm) with Rh/CZA reforming catalysts yields an observed reduction in hydrogen concentration, but with the use of E85, the hydrogen concentration begins to rise; we were able to confirm 70 hours of use. We believe this phenomenon to be intimately related to the fact that ethanol is an oxygen-containing substance.

Next, **Fig. 19** shows the results of measurements of the temperature of the catalytic bed and the SO₂ and CO₂ concentrations during the recovery procedure for E85 and for gasoline (at a reforming temperature of 700°C).

For E85, we see vigorous temperature variations

Table 4 Experimental condition for gasoline concentration.

Catalyst	Rh (4.8 g/L, 9.6 g/L) / CZA (240 g/L)
Support	3 mil / 600 cpsi cordierite honeycomb
Capacity	2 × 0.716 mL (two pieces)
Fuel	E85 (S = 5.0 ppm), E20 (S = 27.2 ppm), Gasoline (S = 34 ppm)
S/C	1.0
GHSV	40000 h ⁻¹
Reforming temperature	600, 700°C
Reforming time	20 min 40 sec
Recovery temperature	550, 650, 700°C
Recovery time	15-35 min
O ₂ concentration (Recovery)	1.0%

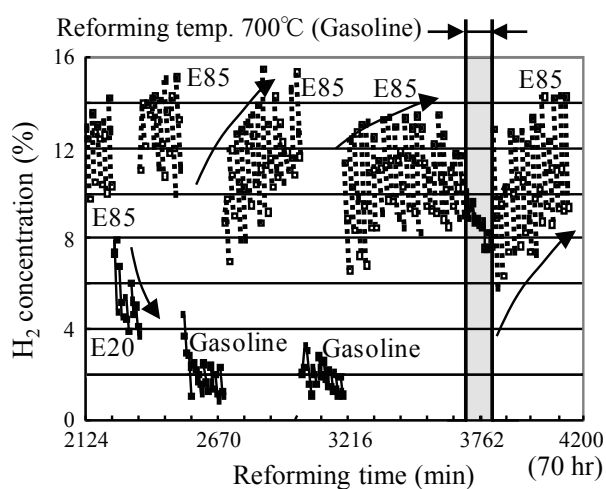


Fig. 18 Effect of gasoline concentration (reforming temp. 600°C, recovery temp. 650°C, S/C = 1.0).

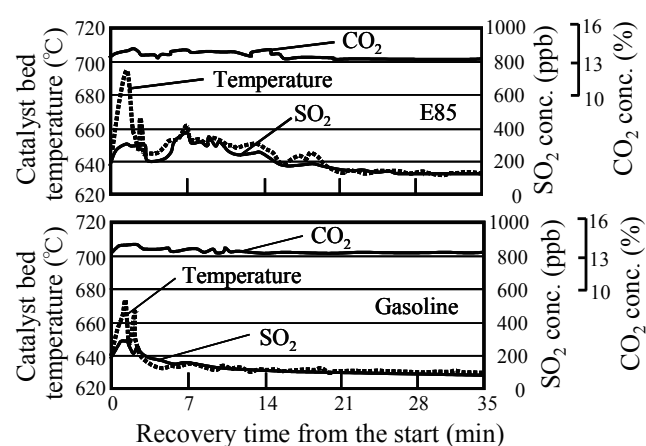


Fig. 19 Behavior of carbon and sulfur in recovery (E85: reforming temp. 600°C, recovery temp. 650°C) (gasoline: reforming temp. 700°C, recovery temp. 650°C).

and emission of CO_2 and SO_2 together with the start of the recovery procedure, and this profile matches the observed variation in the temperature of the catalytic bed. We interpret this finding as an indication that the carbon content of the catalyst dissociates in the form of CO_2 , while the sulfur content dissociates in the form of SO_2 . For gasoline, although there is some rise in the catalytic bed temperature and in the concentrations of CO_2 and SO_2 around the start of the recovery process, the variations are small compared with those for E85 during the first 4 minutes after the start of recovery. For the case of gasoline we found insufficient carbon removal at a recovery temperature of 650°C , suggesting continued degradation of hydrogen-producing performance.

Next, **Fig. 20** shows the results of varying the recovery conditions at a fixed reforming temperature of 700°C using gasoline.

(a) At a recovery temperature of 700°C and an oxygen presence of 1%, the performance persists.

(b) At a recovery temperature of 650°C and zero oxygen presence, the performance is degraded.

(c) At a recovery temperature of 700°C and an oxygen presence of 1%, recovery from the degraded performance is possible.

(d) At a recovery temperature of 550°C and zero oxygen presence, we find significant degradation in performance.

Although not shown in the figure, upon comparing the volumes of carbon and sulfur in the degraded state A in the figure to the volumes after the oxidation recovery process, we found that the sulfur content remained unchanged, while the volume of carbon was overwhelmingly greater in the degraded state.

Based on this finding, we conclude that the factor

- (a) Recovery 700°C , $\text{O}_2 = 1\%$, (b) Recovery 650°C , $\text{O}_2 = 0\%$
 (c) Recovery 700°C , $\text{O}_2 = 1\%$, (d) Recovery 550°C , $\text{O}_2 = 0\%$

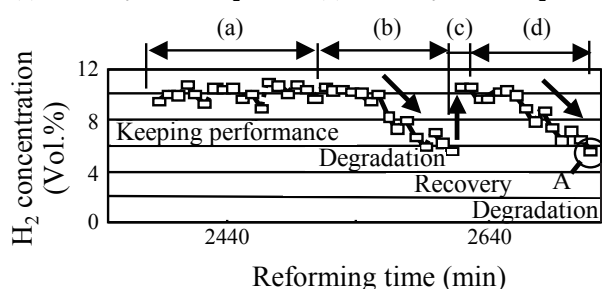


Fig. 20 Degradation and recovery for gasoline use (reforming temp. 700°C).

responsible for the performance degradation is not sulfur, but rather carbon. In addition, when using gasoline, the performance can be recovered at a recovery temperature of 700°C and an oxygen presence of 1%.

Next, with regard to the degradation at A, we performed TPD analysis (room temperature -750°C) under both oxidizing conditions ($\text{O}_2 = 10\%$, residual He) and reducing conditions ($\text{H}_2 = 5\%$, residual He). **Figures 21** and **22** respectively show the rise temperature under the former and latter conditions. In **Fig. 21**, we see two peaks at 350°C and 650°C . The quantity of CO_2 , which is an oxide of carbon, is greatest at the early stages of the catalyst, intermediate at the intermediate stages, and lowest at the later stages. In all regions, the volume of carbon roughly agrees with that observed by carbon and sulfur analyses. In **Fig. 22**, the H_2O peaks arising from the oxidation of hydrogen arise in the range of $100-350^\circ\text{C}$ and above 650°C . We interpret both of these as arising from the emission

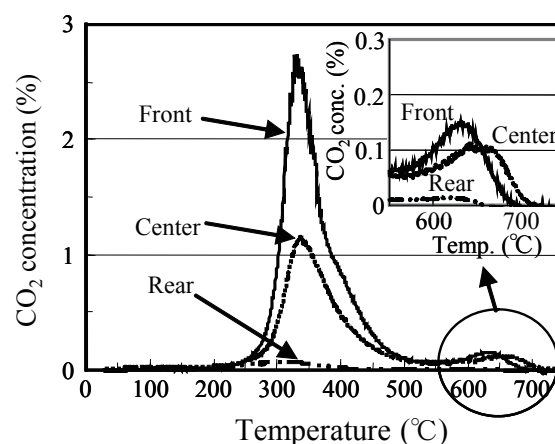


Fig. 21 Behavior of CO_2 in oxidizing atmosphere in TPD.

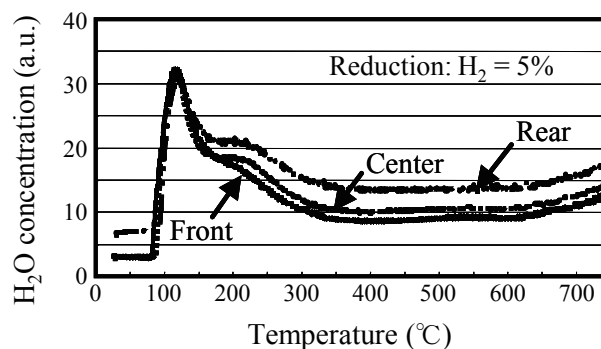


Fig. 22 Behavior of H_2O in reducing atmosphere in TPD.

of oxygen atoms in the ceria lattice. In particular, we take this as evidence linking the use of oxygen in ceria lattices above 650°C to the removal of carbon by oxygen – that is, to the robustness of oxygen activation – observed at a recovery temperature of 700°C in our evaluations of gasoline.

4. Conclusions

In this report, we reported the results of experiments and practical tests involving prototype gasoline engines designed to improve fuel economy by reforming steam from ethanol-blended gasoline. We also analyzed the factors responsible for the degradation and recovery of reforming catalyst, which play an important role in steam-reforming performance, and proposed a new recovery method based on this analysis. Our most important conclusions may be summarized as follows:

(1) Through steam-reforming experiments using EGR in an engine with Rh catalysts (with CaZrO₂ carriers) chosen as reforming catalysts, we succeeded in increasing the volume of EGR introduced through the addition of hydrogen-containing reforming gas, and we confirmed that the fuel economy improved. At intermediate engine speeds and moderate loading, the EGR ratio grew as high as 28%, offering a 4.6% improvement in fuel economy. We attribute this result to the increased heating value due to the recycling of waste heat and to improvements in flame propagation speed due to hydrogen.

(2) We confirmed that the use of CZA as a catalyst carrier yielded a 15% increase in hydrogen production during engine EGR reforming as compared to the use of CaZrO₂ carriers. We expect that further improvements in fuel economy are possible. Considering the simplicity of the procedure needed to recover from degradation, we conclude that the use of this new catalyst carrier is effective for steam reforming using engine EGR.

(3) We believe the factor responsible for degrading the hydrogen-producing performance of the reforming catalyst is not sulfur, but rather carbon sedimentation. When oxygen was supplied at temperatures of 650°C or below during the recovery procedure, the sulfur component of the catalyst remains unchanged, but the carbon component was eliminated, allowing the recovery of hydrogen-producing performance. When CZA was used as a catalyst carrier, the oxygen concentration was 0.5% during the recovery procedure,

and the hydrogen recovery ratio rose to 100% at a temperature of 550°C.

(4) For the Rh/CZA reforming catalyst, the use of gasoline (with sulfur content 34 ppm) degraded the oxygen-producing performance, but the use of E85 (with sulfur content 5.0 ppm) yielded a recovery of hydrogen-producing performance. Moreover, recovery from the degradation caused by the use of gasoline is possible at a temperature of 700°C and an oxygen concentration of 1%. We demonstrated that the hydrogen-producing performance can persist for usage intervals up to 70 hours.

References

- (1) Miyakojima Bio-ethanol Project, <http://www.sangiin.go.jp/japanese/annai/chousa/rippou_chousa/backnumber/2008pdf/20080514060.pdf> (in Japanese), (accessed 2008/08/08).
- (2) Akita prefecture, <<http://pref.akita.lg.jp/www/contents/1239781224845/index.html>> (in Japanese), (accessed 2009-04-15)
- (3) Sumiyoshi, M. et al., “Effect of Alcohol Reformed Gas on Automotive Gasoline Engine”, *JSAE Trans.* (in Japanese), Vol. 100, No. 17 (1979), pp. 32-39.
- (4) Saito, T., “*Nenryou Kaishitsu niyoru Hibanatenkakikan no Netsukouritsukoujou*”, *Nainen-kikan* (in Japanese), Vol. 22, No. 16 (1983), pp. 28-36.
- (5) Okada, O., “*Koujidatsuryuugijutsu no Kaihatsu to Sono Ouyou*”, *Petrotech* (in Japanese), Vol. 20, No. 4 (1997), pp. 345-349.
- (6) Deluga, G. A. et al., “Renewable Hydrogen from Ethanol by Autothermal Reforming”, *Science*, Vol. 303, No. 5660 (2004), pp. 993-997.
- (7) Haryanto, A. et al., “Current Status of Hydrogen Production Techniques by Steam Reforming of Ethanol: A Review”, *Energy Fuels*, Vol. 19, No. 5 (2005), pp. 2098-2106.
- (8) Nagano, S. et al., “High Efficiency Utilization for Bio-ethanol: Steam Reforming of Wet Ethanol”, *JSAE Ann. Congr. (Spring) Proc.* (in Japanese), No. 42-10 (2010), 20105070.
- (9) Hatanaka, M. et al., “Reversible Changes in the Pt Oxidation State and Nanostructure on a Ceria-based Supported Pt”, *J. Catal.*, Vol. 266, No. 2 (2009), pp. 182-190.
- (10) Yamazaki, K. et al., Japanese Patent No. 4269560 (in Japanese), (2009).
- (11) Yamazaki, K. et al., Japanese Patent No. 5207139 (in Japanese), (2013).

Figs. 1-7 and Table 1

Reprinted from Trans. Soc. Autom. Eng. Jpn., Vol. 43, No. 2 (2012), pp. 325-330, Nagano, S., Yamazaki, K., Mandokoro, Y., Nakada, I. and Yahagi, H., Fuel Consumption Improvement by Engine EGR Reforming with Etanol-blended Gasoline Steam Reforming (in Japanese), © 2012 Society of Automotive Engineers of Japan.

Figs. 8-22 and Tables 2-4

Reprinted from Trans. Soc. Autom. Eng. Jpn., Vol. 43, No. 3 (2012), pp. 679-684, Mandokoro, Y., Nagano, S., Yamazaki, K., Nakada, I. and Yahagi, H., Degradation and Recovery of Reforming Catalyst in Etanol-blended Gasoline Steam Reforming (in Japanese), © 2012 Society of Automotive Engineers of Japan.

Susumu Nagano

Research Fields:

- Thermal Engineering
- Engine Combustion
- Fuel Processing

Academic Degree: Dr.Eng.

Academic Societies:

- The Japan Society of Mechanical Engineers
- Society of Automotive Engineers of Japan

